Polar Geosci , **15**, 89-103, 2002

Characteristics of the Moho as revealed from explosion seismic reflections beneath the Mizuho Plateau, East Antarctica

Mikiya Yamashita[1], Masaki Kanao[2] and Tomoki Tsutsui[3]

[1]*Department of Polar Science, The Graduate University for Advanced Studies, Kaga 1-chome, Itabashiku, Tokyo 173-8515*
[2]*National Institute of Polar Research, Kaga 1-chome, Itabashi-ku, Tokyo 173-8515*
[3]*Institute of Applied Earth Sciences, Faculty of Engineering and Resource Science, Akita University, Akita 010-8502*

Abstract: Seismic exploration was conducted on the Mizuho Plateau, East Antarctica, during the 1999-2000 austral summer season by the 41st Japanese Antarctic Research Expedition (JARE-41) Seismic shot records were obtained with clear arrivals of the later reflected phases by a total amount of 3300 kg dynamite charges in seven explosions along the Mizuho traverse route 180 km in length The purpose of this study is to investigate characteristics of the Moho discontinuity from reflective evidence by using explosive seismic waves First, we used the mirror image method for the travel time data of Moho reflected waves (*PmP* phases) Optimal image points were determined to minimize root-mean-square residuals between the observed and the calculated travel times by an iterative grid search at 1 km intervals The depth of the reflected Moho and the averaged incident angles were determined by taking the *P* wave velocity of the crust as a parameter The obtained Moho depth and the associated dipping angle were well correlated with those from the previous reflection study Amplitude spectrum analysis was also applied to obtain the difference in peak frequency of the spectrum between the *PmP* phases and the direct *P* phases The observed spectral ratios of the reflected *PmP* phases to the direct *P* phases indicate spectral peaks at 9 5 and 19 0 Hz, and a spectral trough at 13 8 Hz, respectively This pair of spectral peaks and the trough can be explained by the existence of a thin reflecting layer of 690-860 m thickness just beneath the Moho discontinuity The thin layer may have relatively lower velocities of 7 0-7 8 km/s than those of the surrounding uppermost mantle These relatively low velocity layers around the Moho are considered to be composed of clino-pyroxenite and/or pyroxene-hornblende gneiss by comparison with high-pressure laboratory measurements of metamorphic rocks from the Lutzow-Holm Complex

key words Mizuho Plateau, reflected phases, mirror image method, amplitude spectrum ratio, Moho structure

1. Introduction

The deep crustal structure of the East Antarctic shield is important in relation to the

continental growth process in the Earth's evolution In order to reveal the lithospheric structure and evolution process from Western Enderby Land to Eastern Dronning Maud Land, the project "Structure and Evolution of the East Antarctic Lithosphere (SEAL)" has been carried out since the 1996-1997 austral summer season in the framework of the Japanese Antarctic Research Expedition (JARE) Several geological and geophysical studies including deep seismic surveys have been conducted from the Archean Napier Complex to the early-Paleozoic Lutzow-Holm Complex (LHC) (Shiraishi *et al*, 1994)

In the austral summer season of 1999-2000 (by JARE-41), deep seismic probing was conducted on the ice sheet of the northern Mizuho Plateau (Miyamachi *et al*, 2001, Fig 1) More than 160 geophones with natural period of 2 Hz were planted along the oversnow traverse route from Syowa Station to Mizuho Station, hereafter referred to as the Mizuho route A total charge of 3300 kg of dynamite, detonated at seven sites along the route, could yield seismic signals concerning the deep structure of the continental margin of the LHC Tables of travel times for the first arrival phases from the seven explosions are summarized by Miyamachi *et al* (2001) By using these data, velocities of the uppermost crust and reflecting section down to 20 s of the two way travel time (TWT) were obtained by Tsutsui *et al* (2001a) and Tsutsui *et al* (2001b), respectively

In order to investigate the heterogeneity of the crust and the uppermost mantle from seismic reflected waves, it is important to estimate the distribution of reflectors and averaged velocity model of the surrounding medium However, it is difficult to obtain dips and true velocities of such reflectors only from seismic reflection surveys when the seismic profile has a crooked-line geometry Matsumoto and Hasegawa (1996) developed a mirror image

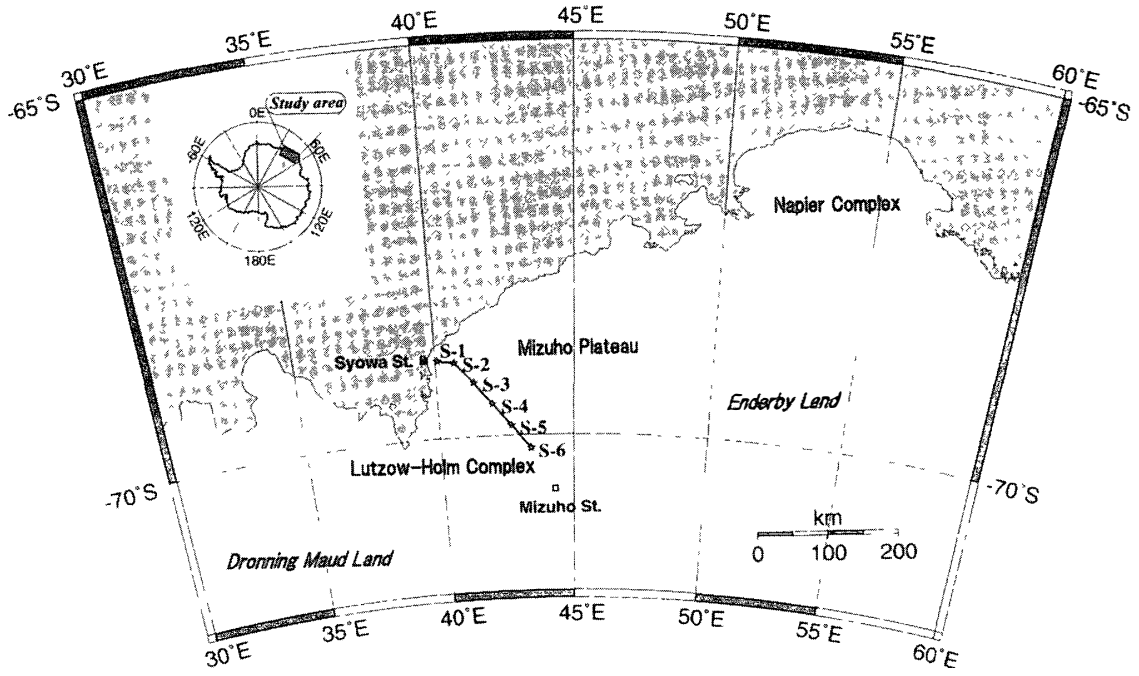

Fig 1 A map showing the seismic survey line by JARE-41 Solid stars indicate the shot points, and the black line shows the seismic line on which 160 geophones were set with an average spacing of 1 2 km

method in order to overcome the above difficulty and estimated locations of crustal reflectors in the volcano area They also applied the amplitude spectral ratio of the reflected S waves to the direct S waves and bound that the reflecting bodies are composed of two thin layers with extremely low S wave velocities On the other hand, Ake and

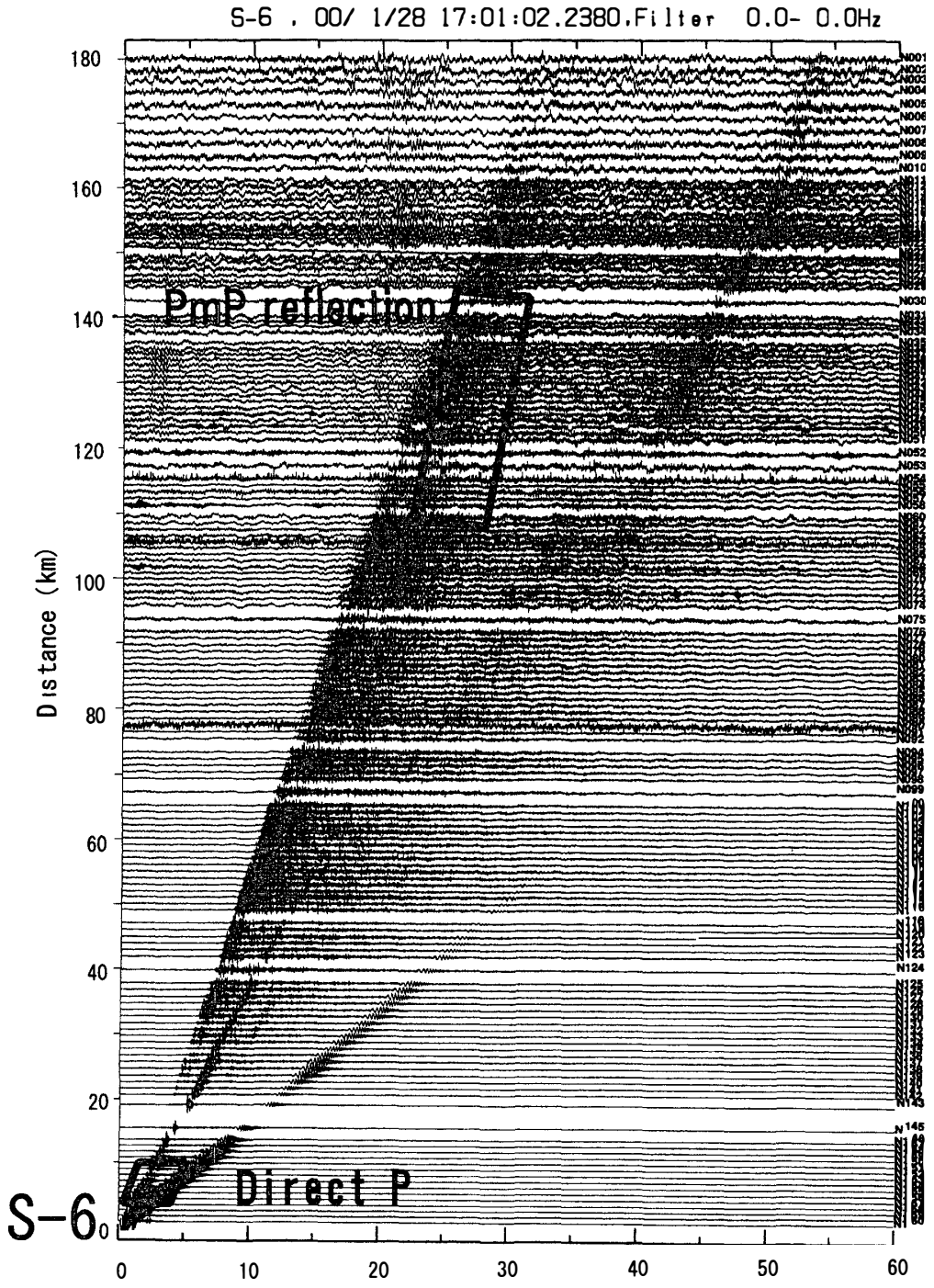

Fig 2 An example of record section (S-6) observed by JARE-41 Each trace is normalized by its maximum amplitude in the trace Two open square markers show the area analyzed by the mirror image method and spectral analysis

Sanford (1988) estimated the thickness of thin (<150 m) magma bodies by modeling the stacked spectra of *PxP* phases from the frequency characteristics of the apparent reflection coefficient

In this study, we adopted a similar mirror image method for the travel time data of Moho reflected waves (*PmP* phases) to obtain the accurate location of the Moho discontinuity beneath the Mizuho route Fig 2 shows an example of *PmP* phases by a shot record (S-6) observed by the JARE-41 seismic experiment (Miyamachi *et al*, 2001) These Moho reflection phases can be clearly observed at thirty stations within the epicentral distance of 110-140 km from the shot point S-6 Then, amplitude spectrum ratio analysis was applied for the combination of the *PmP* phases and the direct *P* phases We focused on the inner structure of the Moho discontinuity in relation to features of laminated layers and metamorphic rock velocities

2. Mirror image analysis

Figure 3 schematically illustrates the applied mirror image method Seismic rays from the source to the reflector can be regarded as coming from the image point of the source, the equivalent of direct rays from the image point to the geophones Here we assumed straight ray paths by assuming constant velocity within the layer between the reflector and the surface Reflected points were assumed to be located on the same plane, and the optimum location of the reflector (reflection point) was estimated from travel time data at the above-mentioned thirty stations An image point was assumed within the restricted region for an assumed velocity of the reflected waves, such as 6 2 km/s, and the theoretical travel time for the image point was calculated The most likely position of the image point was determined when the residual between the calculated travel time and the observed travel time takes a minimum value Such as RMS residual for minimizing error can be written as,

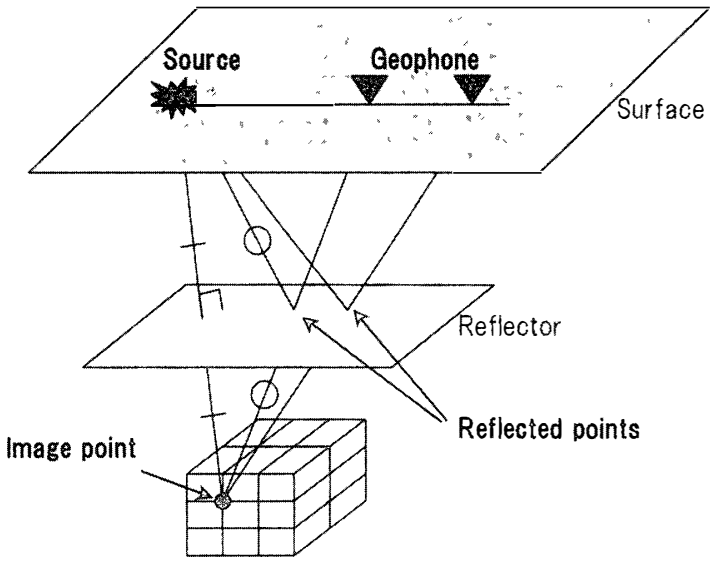

Fig 3 Schematic illustration of ray paths of PmP phases and location of the image point with respect to the reflector

$$S_j=\sum_{i=1}^{N}[t_{ij}-\sqrt{(x_i-x_j)^2+(y_i-y_j)^2+(z_i-z_j)^2}/V]^2, \quad (1)$$

where t_{ij} is travel time at the reflected wave, x_i, y_i, z_i are coordinates of the geophone location, x_j, y_j, z_j are those of the estimated image points with location of jth shot and V is averaged velocity of the reflected wave from surface to reflector The spatial extent of the search region for the image point was bounded in the range of 20–200 km, with 1 km spacing The estimated reflector is perpendicular to the ray path connecting the source and its mirror image, which will give us an estimate of the dipping angle of the reflector Arrival times for the *PmP* phases were picked from the onsets of maximum amplitude arrivals (see triangles in Fig 4) After trial-and-error approximation, location of the reflected Moho discontinuity was determined by assuming a crustal velocity in the range of 6 0–6 4 km/s at intervals of 0 1 km/s

The obtained Moho depth and dipping angles are illustrated in Fig 5a for the five assumed plausible crustal velocities Some schematic rays are plotted from shot point (S-6) to several stations (N026–N064) for the case of estimated reflectors A grid search was carried out in the three-dimensional field However, the seismic profile from S-2 to S-6 is basically two-dimensional, thus the results are simply expressed two-dimensionally The Moho depth with the assumed crustal velocity of 6 0–6 3 km/s is consistent with those found in previous refraction studies on the Mizuho route by JARE-21 (Ikami *et al*, 1984, Ikami and Ito, 1986) If we assume a 6 4 km/s velocity, which corresponds to that in the middle crustal layer found by Ikami *et al* (1984), the Moho depth becomes deeper, around 45–50 km, than that found in the refraction analysis by JARE-21 On the other hand, the obtained Moho reflection points for the 6 2 km/s crustal velocity are comparable with the

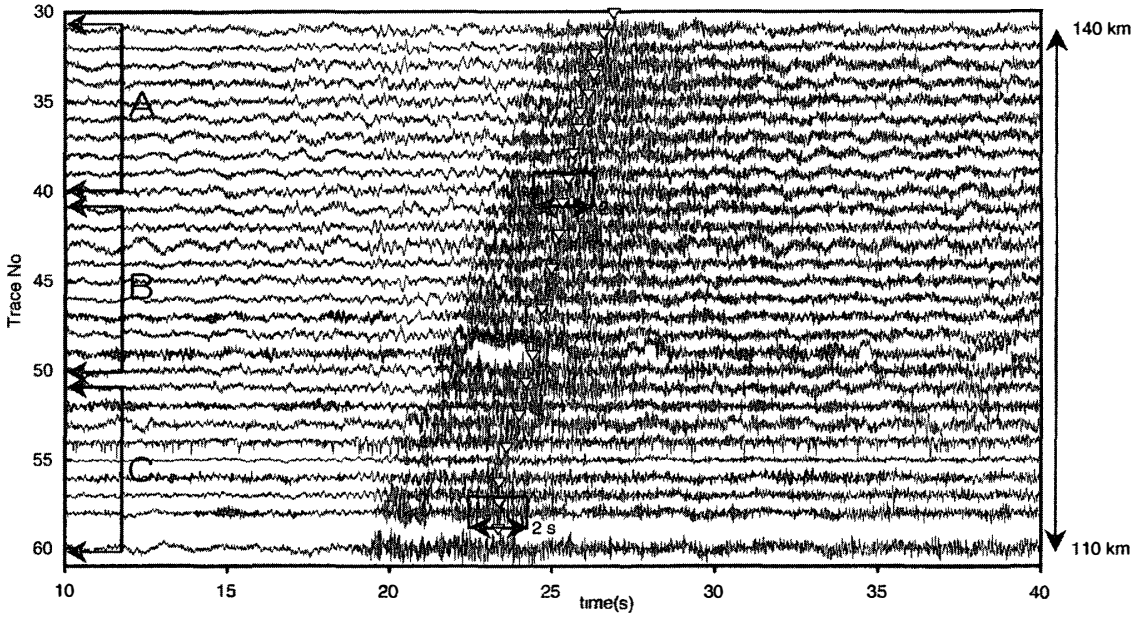

Fig 4 A shot record for PmP phases Each trace is normalized by the maximum amplitude in the trace Two open squares are the examples of 2 s window of spectral analysis for PmP phases A, B and C indicate station numbers N031–040, N041–N050 and N051–N060, respectively

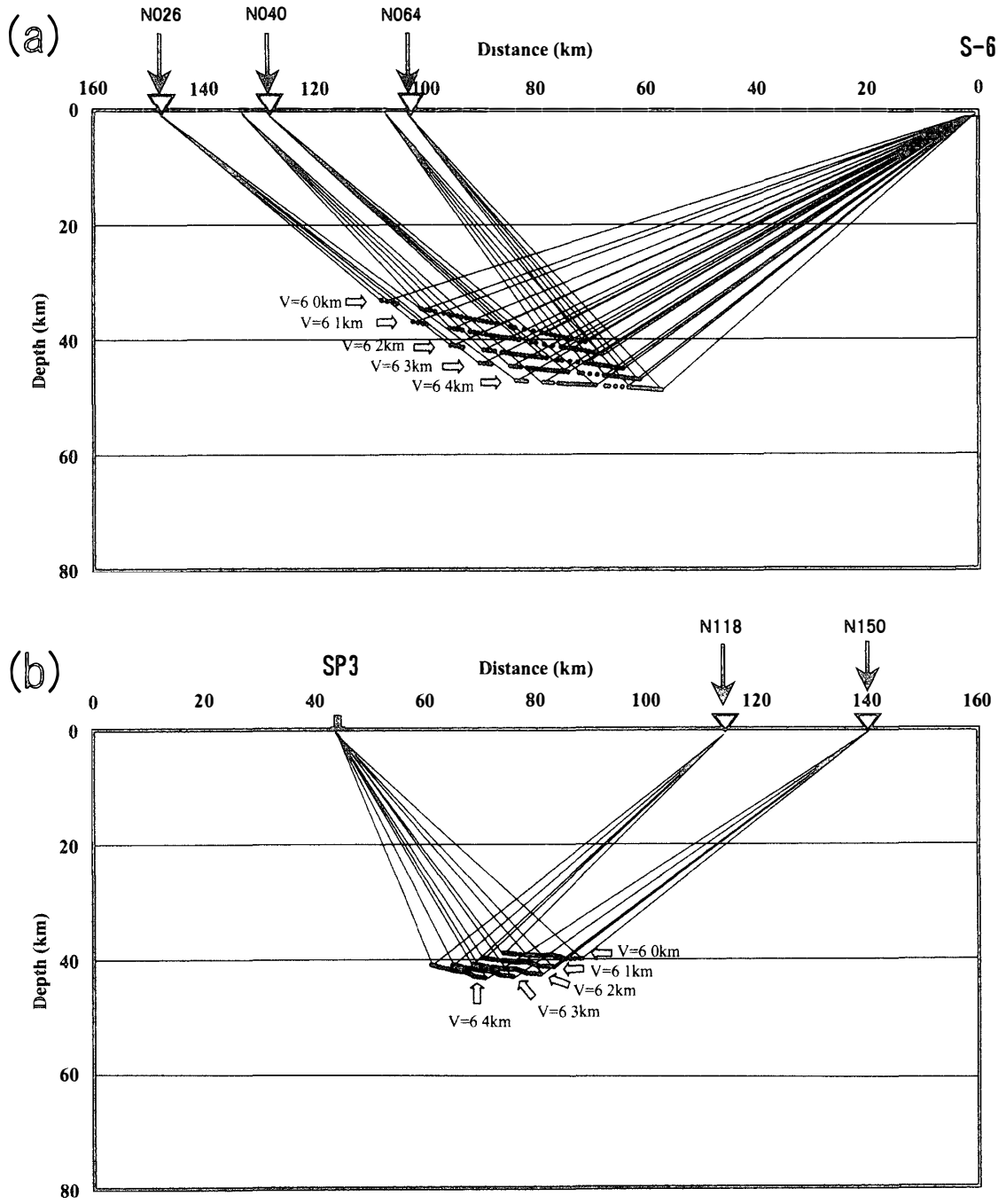

Fig 5 *The results of a grid search using the mirror image method for five assumed crustal velocities (a) Some of the rays are plotted from the shot point (S-6) to several stations (N026-N064) from Moho reflection for several reflected velocities (b) Some of the rays are plotted from the shot point (S-3) to several stations (N026-N064) from Moho reflection for several reflected velocities*

reflection sections of Tsutsui *et al* (2001b) In Fig 5b, the location and dipping angles of the Moho are well correlated with the results beneath the S-4 region, in the central part of the seismic survey line This implies that the averaged RMS velocity in the crust by reflection analysis is nearly uniform, around 6 2 km/s, in the mid-crustal depth range

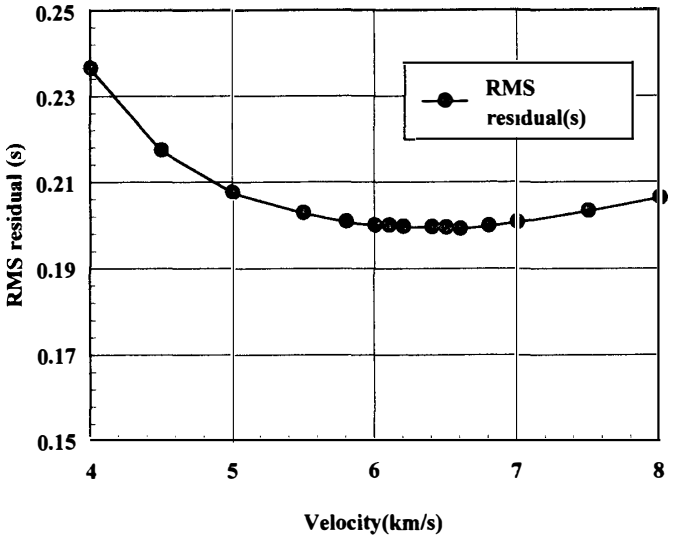

Fig 6 RMS residuals plotted for assumed velocities for grid search in the mirror image method for shot point S-6

When V becomes smaller, the depth of the reflecting plane becomes shallower with an enhanced dip toward the inland direction For $V=6.0$ km/s, the depth of the reflecting plane at N064 is 35 km with the associated dipping angle of 10° For $V=6.4$ km/s, the corresponding values are 46 km and 3°, respectively This trade-off between the assumed crustal velocity and the Moho depth comes from the uncertainty in the determination of absolute velocities in the reflected phase analysis Figure 6 shows the variation of total RMS residuals versus velocity The residuals are insensitive to the value of V and almost flat for the variation range between 6.0 and 6.4 km/s, and it is rather difficult to optimize V from the convergence curve However, we adopt here $V=6.2$ km/s as the most appropriate value from comparison with the previous refraction studies by JARE-21 (Ikami *et al*, 1984, Ikami and Ito, 1986) and the reflection analysis by Tsutsui *et al* (2001b), because it gives the value of about 40 km Moho depth at N064 and the associated dip angle of 7°

3. Amplitude spectrum analysis

For a thin layer with different velocity than the surrounding medium, reflections from the top and the bottom of the thin layer (see Fig 7) may result in constructive/destructive interferences depending on the relationship among incident angle, thickness and wave length In this study, however, incident angles at the Moho vary insignificantly against a small epicentral distance range, the incident angle at the Moho is approximately 60° from the result of the mirror image method (Fig 5) Reflected waves become strong when a top reflection is in phase with a bottom reflection, weak when a top reflection is out of phase with a bottom reflection, similarly to the interference of light In case of vertical incidence to the thin layer, the phase relationship against frequency for the above conditions can be easily formulated, and its characteristic nature produces periodical spectral peaks in the frequency domain The spectrum of reflected waves contains the effect of both internal structure of the reflectors and the source spectrum itself Observed waves can be expressed

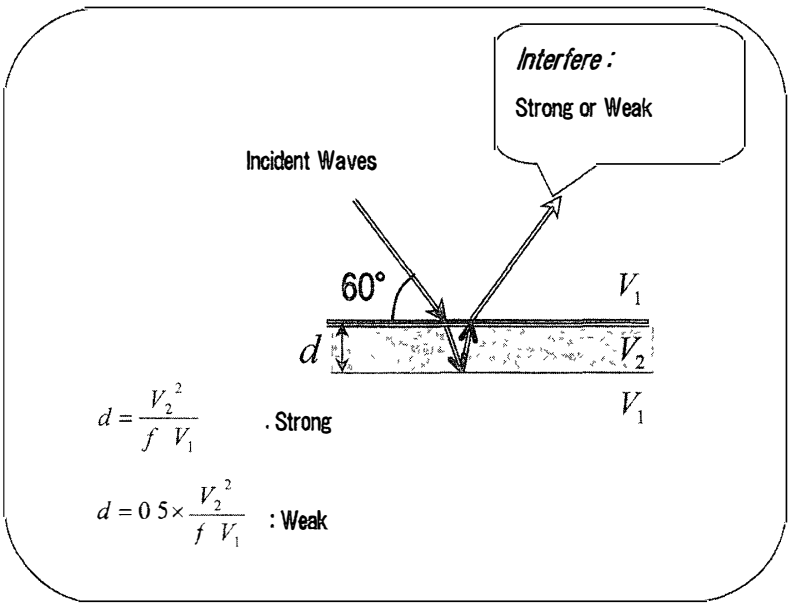

Fig 7 The concept of investigation of the internal structure using reflected waves by interference of a thin layer d is the thickness of the thin layer (m), V_1 is velocity around the reflector and V_2 is the internal velocity of the thin layer

as a convolution of source waves and an impulse response of the reflection coefficient in the time domain Thus an apparent reflection coefficient can be calculated by dividing the spectrum of reflected waves by the spectrum of direct P phases after transformation in the frequency domain

In general, the amplitude spectrum of PmP phases can be written as a function of of frequency f

$$A_{ref}(f) = S(f) \circ H_{ref} \circ I(f) \circ W(f) \circ R(f), \quad (2)$$

where $A_{ref}(f)$ is the spectrum of the observed time series, $S(f)$ is the source function, H_{ref} represents geometrical spreading, $I(f)$ represents instrumental plus site response, $W(f)$ is an attenuation factor, and $R(f)$ is the reflection coefficient at the Moho Though $W(f)$ can be expressed as,

$$W(f) = \exp(-2\pi f \circ t/Q), \quad (3)$$

where t is the travel time of PmP phases, the intrinsic quality factor Q along the ray path is considered as frequency independent, thus $W(f)$ can be considered independent of frequency

Records within 6 km from the shot point give clear direct waves without contamination by head waves and reflected waves (*e g* Tsutsui *et al* , 2001b) Then, the amplitude spectrum $A_{dir}(f)$ for the direct P waves can be expressed as,

$$A_{dir}(f) = S(f) \circ H_{dir} \circ I(f), \quad (4)$$

where H_{dir} represents geometrical spreading of the direct P wave When we take the amplitude ratio of $A_{ref}(f)$ to $A_{dir}(f)$,

$$PmP/P=\frac{A_{\mathrm{ref}}(f)}{A_{\mathrm{dir}}(f)}=W(f)\cdot\frac{H_{\mathrm{ref}}}{H_{\mathrm{dir}}}\cdot R(f), \tag{5}$$

has the same frequency characteristic as that of $R(f)$, that is, it is an apparent reflection coefficient

In this study, these amplitude spectrum analyses were applied to reveal the difference in peak frequency of the spectrum between *PmP* phases and direct *P* phases of body waves Then, reflection coefficients of the Moho discontinuity beneath the Mizuho route were estimated from the above amplitude spectral method Spectra with large enough S/N ratios were obtained after stacking several adjacent spectra, which reduced incoherent noise If reflection coefficients have periodicity for spectral peaks and troughs in the frequency domain, the thickness of a thin layer can be calculated using a simple equation

$$d=\frac{V_2^2}{f\cdot V_1} \tag{6}$$

where d is the thickness of the thin layer, V_1 is the velocity around the reflector, V_2 is the velocity within the thin layer, and f is the periodic interval of the spectral peaks If f of a periodic interval of the spectral peaks and trough and V_1 are known, d is calculated by giving V_2 In this study, we observed the spectral peak interval of 9 5 Hz, which was substituted into eq (6)

Figure 8 shows record section of direct *P* waves for S-6 Figure 9 shows an example of the stacked spectrum for the direct *P* phases observed for shot S-6 A total of six records (N151–N156) were stacked to produce an enhanced spectrum peak around 33 Hz (Fig 9b) On the other hand, the spectrum peaks for *PmP* phases (Fig 4) exist around

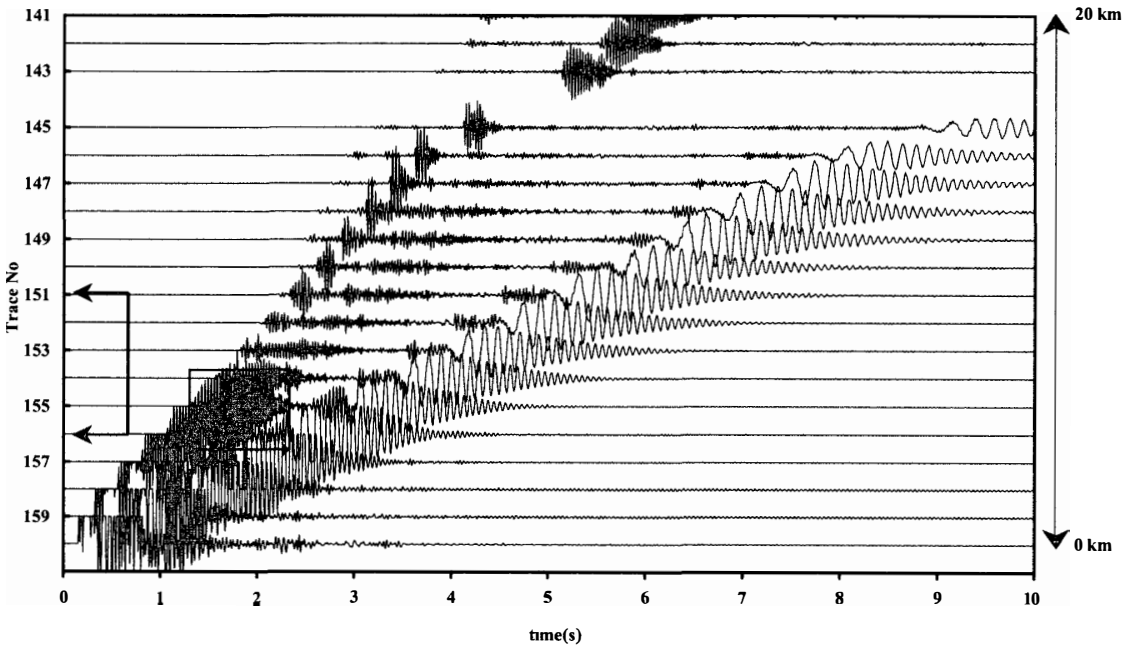

Fig 8 Record section of direct P waves for S-6 Each trace is normalized by the maximum amplitude in the trace An area of open square is a 1 s window of spectral analysis for the direct P phases (N151–N156)

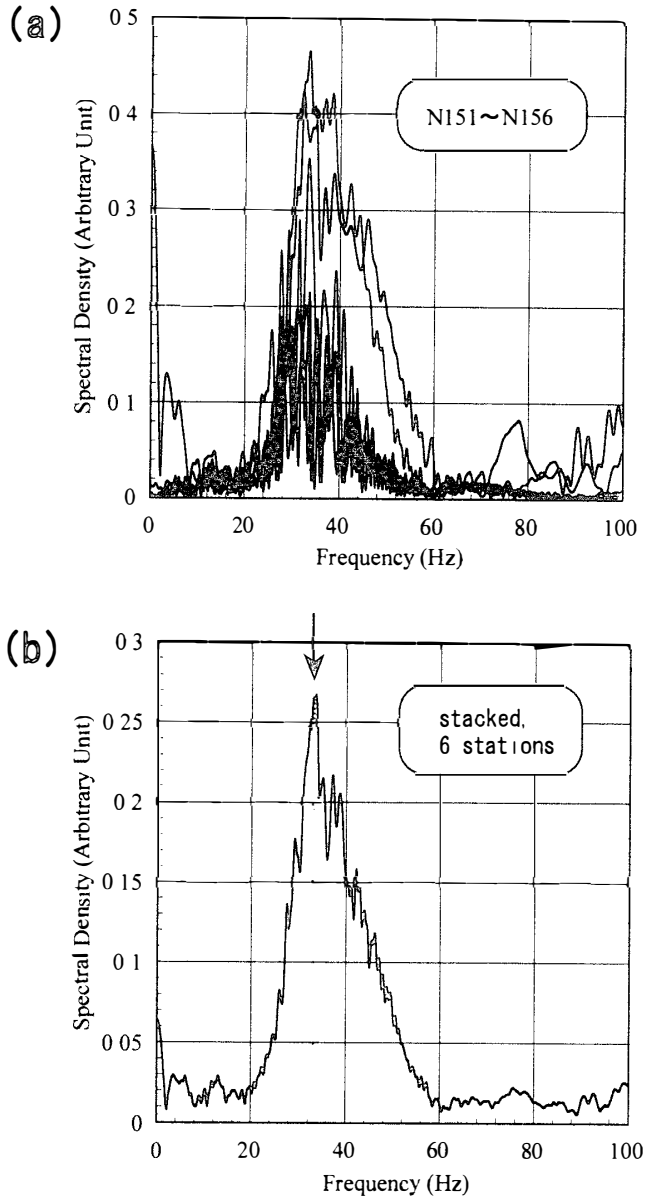

Fig 9 (a) Amplitude spectrum of direct P wave from the explosion source for each trace N151-156 (b) Amplitude spectrum of direct P waves stacked for six stations in Fig 9a

both 8 Hz and 21 Hz, for the stacked record numbers of N031-040, N041-050 and N051-060, respectively as shown by solid curves in Figs 10a-c, where dotted curves correspond to noise spectra and have no significant peaks or troughs Then relatively low frequency peaks were enhanced in the *PmP* spectrum rather than those in the spectrum of direct *P* waves For both analyses, time windows for spectrum analysis were taken as 10 s for direct *P* phases (Fig 8) and 20 s for the *PmP* phases (Fig 4), respectively And the spectral frequency range was bounded within 5-25 Hz Eventually, we obtained the spectral ratios of *PmP* phases to direct *P* phases for the three epicentral groups shown in Fig 10 The results in Figs 10d-f reveal the pair of spectral peaks at 9 5, 19 0 Hz and the spectral trough at 13 8 Hz, respectively The other strong peaks such as 8, 11, 21 Hz cannot be explained by the reflected wave interaction

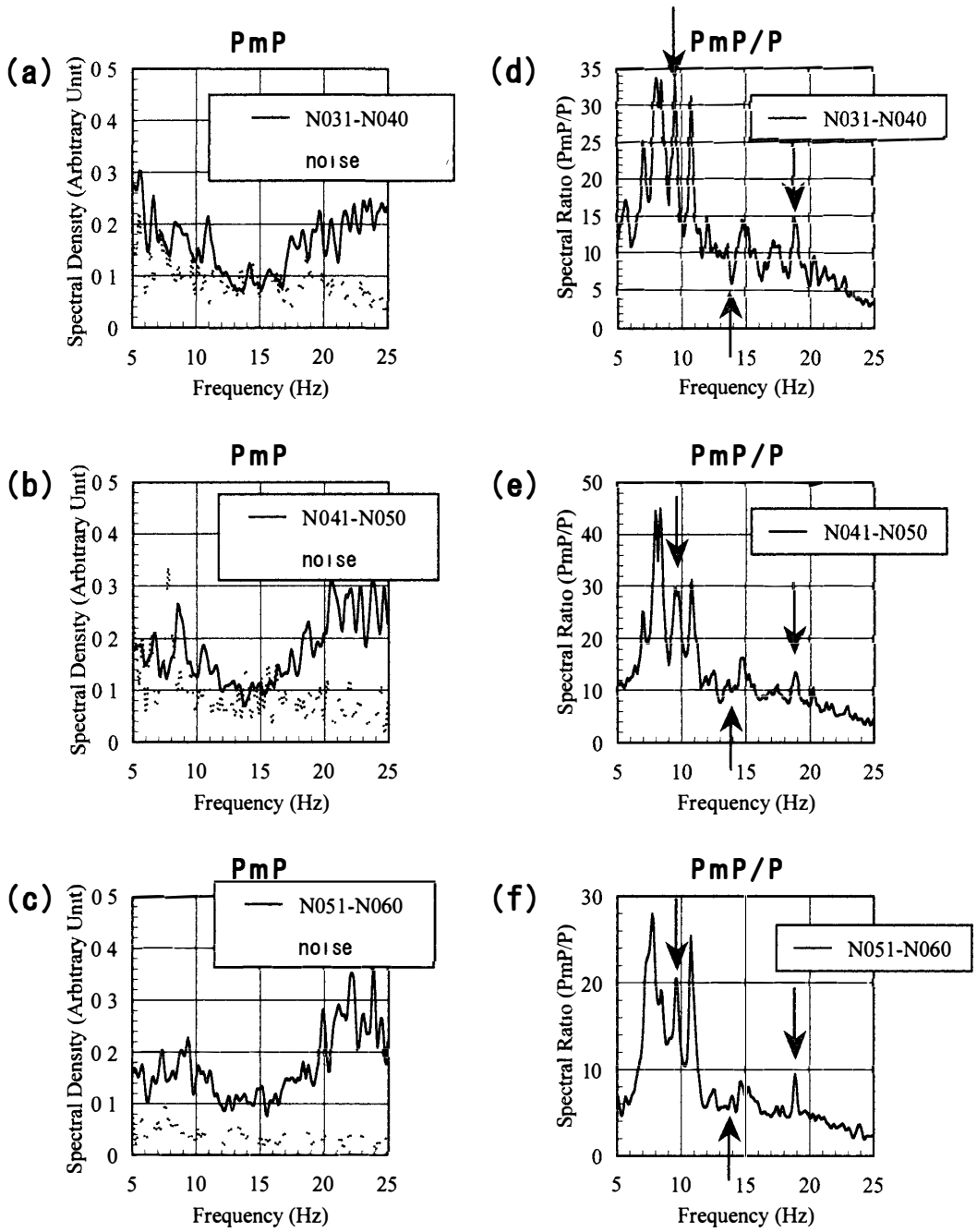

Fig 10 *(a)-(c) Amplitude spectrum of noise and PmP phases stacked for ten traces from stations N031 to N060 (d)-(f) Spectral ratio for PmP to direct P phases of ten traces from stations N031 to N060*

Since f in eq (6) was obtained as 9 5 Hz from the spectral ratio analysis, the thickness of the thin layer d can be estimated by taking the associated velocity V_2 as a parameter, because the V_1 was obtained as 7 9 km/s Table 1 presents several models of thickness patterns of this thin layer calculated by a formula (6) If we assume the relatively low velocities of the thin layer as 7 0–7 8 km/s comparing with the surrounding uppermost mantle, then the thickness of the layer would become about 690–860 m On the other hand, in the case of relatively high velocities of 8 0–8 2 km/s in the thin layer, the thickness

Table 1 Thickness of a thin layer as a function of assumed velocity from 7.0–8.2 km/s

Velocity (km/s)	Thickness of thin layer (m)
7.0	690
7.2	730
7.4	770
7.6	810
7.8	860
8.0	900
8.2	950

would become about 900–950 m

4. Discussion

For the Moho transitional boundary, several laminated multi-layer models are reported and/or proposed. A petrological model of the averaged velocity-depth profile for the continental crust has been presented as a mixed composition of common rock types (Christensen and Mooney, 1995). Reflection densities in the vertical cross section are also calculated in the lower crustal and the upper most mantle as originated from metamorphic layering for those common rock types, for instance by a couple of amphibolite and mafic granulite. Enderle *et al.* (1997) presented the transitional structure of the crust-mantle boundary by fitting the observed *PmP* phases with the synthetic record section for deep seismic probing in Russia. Regarding the Mizuho Plateau, on the contrary, lower crustal-upper mantle strong reflections has already been reported from the normal-move-out (NMO) results in 8–15 s of TWT by Ito and Kanao (1996). A reflective lower crust in LHC has also been suggested by fitting synthetic receiver functions to the observed ones around Syowa Station (Kanao, 1997).

We discuss here physical properties of the thin layer around the Moho in relation to rock composition from the interpretation of the spectral ratio analysis. From the high-pressure experiments on metamorphic rocks, higher velocities than 8.0–8.2 km/s around the crust-mantle boundary depth cannot be explained from the composition of existing rock minerals. The crust-mantle boundary will consist of a mixture of relatively lower velocity (7.0–7.8 km/s) lower crust materials and relatively higher velocity (7.9 km/s) uppermost mantle minerals. In Fig. 11, low velocity region estimated from the spectral ratio analysis (squared area) is superposed on the V_p model obtained from the JARE-21 refraction study (Ikami and Ito, 1986). In order to explain the predominant low velocity range, lamination and/or contamination from the lower crustal materials (less than 6.9 km/s) to the uppermost mantle (7.9 km/s) may be reasonable.

P wave velocity measurements of the high-grade metamorphic rocks from LHC and the surrounding tectonic terrains under high pressure (~1.0 Gpa) have recently been conducted by Shingai *et al.* (2001) and Kitamura *et al.* (2001). The obtained *P* wave velocities 1.0 Gpa at room temperature were 7.28 km/s and 7.29 km/s for clino-pyroxenite and pyroxene-hornblende gneiss, respectively, as summarized in Table 2 of Kitamura *et al.* (2001). The relatively low velocity layers with 7.0–7.8 km/s around the Moho discontinu-

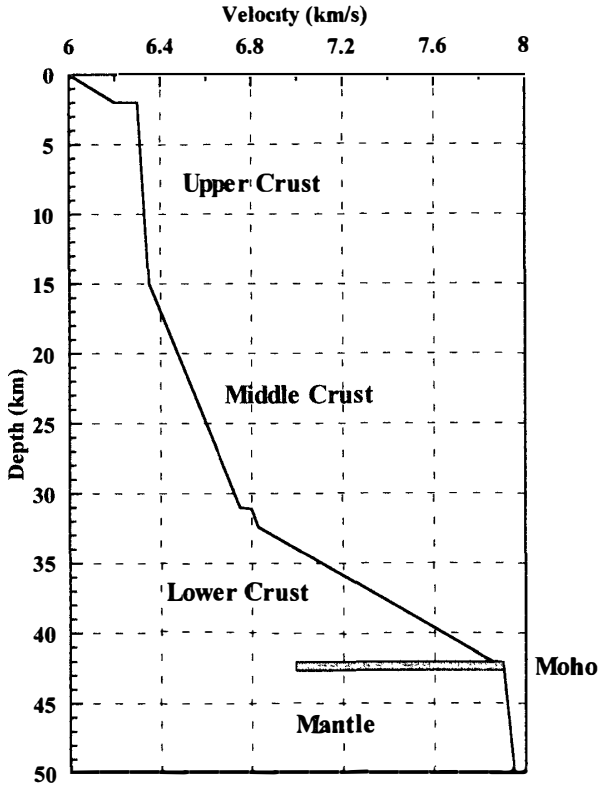

Fig 11 Velocity structure from refraction analysis by Ikami and Ito (1986) plotted on the thin layer estimated from this study

Table 2 P-wave velocities under various pressure conditions for metamorphic rocks from LHC (referred from Kitamura et al, 2001)

Pressure (GPa)	Clino-pyroxenite	2Px amphibolite	Px-Hb gneiss	Hb gneiss	Calc-silicate gneiss
0 6	7 241	6 797	7 157	6 695	6 198
0 8	7 253	6 983	7 269	6 737	6 340
1 0	7 279	7 027	7 228	6 910	6 404

Pressure (GPa)	Felsic gneiss1	Felsic gneiss2	Bt-Opx-Hb granulite	Bt-2Px granulite
0 6	6 526	6 158	6 495	6 583
0 8	6 590	6 234	6 536	6 639
1 0	6 608	6 269	6 786	6 684

(velocity is in km/s)

ity may be explained by the existence of metamorphic rocks such as clino-pyroxenite and/or pyroxene-hornblende gneiss As an alternate explanation, rocks having rather lower velocities such as hornblende gneiss (V_p=6 91 km/s at 1 0 GPa) and biotite-two-pyroxenite granulite (V_p=6 68 km/s at 1 0 GPa) may have contaminated into high velocity mantle materials Studies on the detailed structure of the Moho discontinuity in relation to the lamination/contamination will be extended by an application of our spectral ratio method to Moho reflected waves in further seismic explosion experiments

5. Conclusions

Geometrical features (depth, dip, etc) and inner structure of the Moho discontinuity beneath the Mizuho traverse route were investigated by analyzing Moho reflected waves (*PmP* phases) observed with the JARE-41 seismic array The main results are summarized as follows

1) The mirror image method was applied to travel time data of the Moho reflected waves (*PmP* phases) The depth of the reflected Moho and averaged dip angles were determined by assuming the uniform velocity within the crust to be 6 2 km/s, the most plausible values (40 km and 7°) agreed well with those from the reflection study by Tsutsui *et al* (2001b)
2) The internal structure of the Moho transition zone was estimated from amplitude spectral ratios of *PmP* phases to the direct *P* phases in the near field records Observed spectral ratios reveal spectral peaks at 9 5 and 19 Hz and a trough at 13 75 Hz, respectively This peak-trough pattern could be explained by a thin reflected layer 690–860 m in thickness just beneath the Moho discontinuity The thin layer might have relatively lower velocity of 7 0–7 8 km/s than those of the surrounding uppermost mantle (7 9 km/s, after Ikami and Ito, 1986) Then this layer could be explained by contamination of lower crustal metamorphic rocks with high velocity mantle materials

Acknowledgments

We sincerely thank Prof K Ito of Kyoto University and Prof K Shibuya of NIPR for their suggestions and critical review of the manuscript The authors also sincerely thank JARE-40, and -41 related members, particularly for Prof H Miyamachi of Kagoshima University and Prof S Toda of Aichi Educational University, for their great efforts to obtain seismic survey data on the Mizuho route

References

Ake, J P and Sanford A R (1988) New evidence for the existence and internal structure of a thin layer of magma at mid-crustal depths near Socorro New Mexico Bull Seismol Soc Am **78** 1335–1359

Christensen N I and Mooney, W D (1995) Seismic velocity structure and composition of the continental crust A global view J Geophys Res **100** 9761–9788

Enderle U Tittgemeyer M Itzin M Prodehl C and Fuchs K (1997) Scales of structure in the lithosphere—images of processes Tectonophysics **275** 165–198

Ikami, A and Ito, K (1986) Crustal structure in the Mizuho Plateau East Antarctica by a Two-Dimensional Ray Approximation J Geod **6**, 271–283

Ikami A Ito, K Shibuya, K and Kaminuma K (1984) Deep crustal structure along the profile between Syowa and Mizuho Stations, East Antarctica Mem Natl Inst Polar Res , Ser C (Earth Sci), **15** 19–28

Ito, K and Kanao, M (1996) Detection of reflected waves from the lower crust on Mizuho Plateau, East Antarctica Nankyoku Shiryô (Antarct Rec), **39**, 233–242

Kanao, M (1997) Variations in the crust structure of the Lutzow-Holm Bay region East Antarctica using shear wave velocity Tectonophysics, **270** 43–72

Kitamura, K , Ishikawa M Arima, M and Shiraishi K (2001) Laboratory measurements of *P*-wave

velocity of granulites from Lutzow-Holm Complex, East Antarctica Preliminary report Polar Geosci , **14**, 180-194

Matsumoto, S and Hasegawa, A (1996) Distinct *S* wave reflector in the midcrust beneath Nikko-Shirane volcano in the northeastern Japan arc J Geophys Res , **101**, 3067-3083

Miyamachi, H , Murakami, H , Tsutsui, T , Toda, S , Minta, T and Yanagisawa, M (2001) A seismic refraction experiment in 2000 on the Mizuho Plateau, East Antarctica (JARE-41)—Outline and observations— Nankyoku Shiryô (Antarct Rec), **45**, 101-147 (in Japanese with English abstract)

Shingai, E , Ishikawa, M and Arima, M (2001) *P*-wave velocity in ultrahigh temperature granulites from the Archean Napier Complex, East Antarctica Polar Geosci , **14**, 165-179

Shiraishi, K , Ellis, D J , Hiroi, Y , Fanning, C M , Motoyoshi, Y and Nakai, Y (1994) Cambrian orogenic belt in East Antarctica and Sri Lanka Implications for Gondwana assembly J Geol , **102**, 47-65

Tsutsui, T , Murakami, H , Miyamachi, H , Toda, S and Kanao, M (2001a) *P*-wave velocity structure of the ice sheet and the shallow crust beneath the Mizuho traverse route, East Antarctica, from seismic refraction analysis Polar Geosci , **14**, 195-211

Tsutsui, T , Yamashita, M , Murakami, H , Miyamachi, H , Toda, S and Kanao, M (2001b) Reflection profiling and velocity structure beneath Mizuho traverse route, East Antarctica Polar Geosci , **14**, 212-225

(Received April 25, 2002, Revised manuscript accepted July 3, 2002)